Self-Ordered Anodic Alumina with Continuously Tunable Pore Intervals from 410 to 530 nm

Chuanmin Sun,[†,‡] Jia Luo,[†,‡] Longmin Wu,[*,†] and Junyan Zhang[*,‡]

State Key Laboratory of Applied Organic Chemistry, College of Chemistry and Chemical Engineering, Lanzhou University, Lanzhou 730000, China, and State Key Laboratory of Solid Lubrication, Lanzhou Institute of Chemical Physics, Chinese Academy of Sciences, Lanzhou 730000, China

ABSTRACT We report a "mild anodization" (MA) process using aluminum oxalate (Alox) as an additive to suppress breakdown of porous anodic alumina (PAA) in the electrolyte of phosphoric acid at high potentials and comparatively high temperatures. It is shown for the first time that continuously tunable pore intervals (D_{int}) from 410 to 530 nm with ordered hexagonal pore arrangement can be controlled by varying the concentrations of phosphoric acid and Alox at anodization voltages (U_a) from 180 to 230 V, far beyond the U_a in the single electrolyte of phosphoric acid or oxalic acid. The fabricated PAA films are uniform without any burning spots, and the anodization temperature can be increased to 10−20 °C with a much higher growth rate of PAA films than that at a low temperature. Meanwhile, a typical two-step anodization process could also be performed under our conditions. Our results could not only extend the applications of PAA templates but also facilitate understanding of the effects of anions in the process of anodic oxidation.

KEYWORDS: anodic alumina • pore interval • aluminum oxalate • phosphoric acid • anions effect

As a versatile nanoscale platform, PAA with self-ordered pore arrays has shown lots of advantages in the field of studies on fluidic dynamics in nanoholes (1, 2), fabrication of nanostructure supercapacitors, photoelectric materials (3), separation filters (4), and other nanodevices (5, 6), such as (1) D_{int} controllable by tuning U_a, (2) pore size and aspect ratio adjustable by varying H_3PO_4 etching and anodic oxidation duration, respectively, (3) D_{int} and pore size uniform with straight pore channels, (4) thermostable at very high temperature (melting point: 2050 °C), and (5) low cost with simple preparation procedures.

However, problems still exist in the current fabrication techniques of PAA films. In the conventional MA processes (7, 8), the conditions of anodic oxidation are gentle, and ordered nanopore arrays throughout PAA films can be obtained by using two-step anodization (9), but only several specific D_{int} of PAA films are achieved. In the newly proposed "hard anodization" (HA) process (8, 10, 11), PAA films grow much more quickly with much higher current density than MA, and D_{int} in comparatively wider windows can be accomplished by tuning U_a; however, a very low temperature is required in the anodization process, and some pretreatments of samples, such as preoxidation of aluminum for formation of an uniform oxide layer before the HA process, are essential to suppress the breakdown effect and inhomogeneous growth of PAA films, and two-step anodizaiton is difficult to proceed for HA (12). Thus, a simple and facile fabrication process for self-ordered PAA with continuously tunable D_{int} and a relatively high film growth rate under MA conditions is desired for further improved nanofabrications.

Phosphoric acid is usually employed as the electrolyte for PAA with larger D_{int}, however, the process has to be carried out at the voltage lower than 170 V to avoid the breakdown of PAA films, and ordered hexagonal arrangement of pores with uniform pore size can not be fulfilled. Recently, addition of organic solvents to H_3PO_4 was reported for obtaining self-ordered PAA films (13). However, to the best of our knowledge, the ordered hexagonal pore arrays with continuously tunable D_{int} larger than 400 nm have not been realized yet.

Here we present a highly reproducible approach, employing different concentrations of H_3PO_4 with the addition of Alox, to obtain self-ordered PAA with continuously tunable D_{int} from 410 to 530 nm at U_a from 180 to 230 V, and the film growth rate could be increased to 40−50 μm h^{-1} when anodized at 10−15 °C, in contrast with 8−10 μm h^{-1} at 5 °C. The highly ordered hexagonal pore arrays throughout PAA films have been achieved by using simple two-step anodization. Meanwhile, the role of the oxalate anions in the anodization process has also been discussed.

RESULTS AND DISCUSSION

Anodization was investigated with constant voltage of 205 V at 5 °C to optimize the amount of Alox added in the electrolyte of 1.0 wt % H_3PO_4 for obtaining the self-ordered PAA films. The current−time (I−t) transients show that the current increases with the decreased concentration of Alox (left of Figure 1), and the average current density in the electrolyte with 0.01 M Alox is twice as high as that of 0.02 M Alox, while in the electrolyte with 0.005 M Alox, high

* Corresponding author. E-mail: nlaoc@lzu.edu.cn.
Received for review March 01, 2010 and accepted April 19, 2010
† Lanzhou University.
‡ Chinese Academy of Sciences.
DOI: 10.1021/am1001713

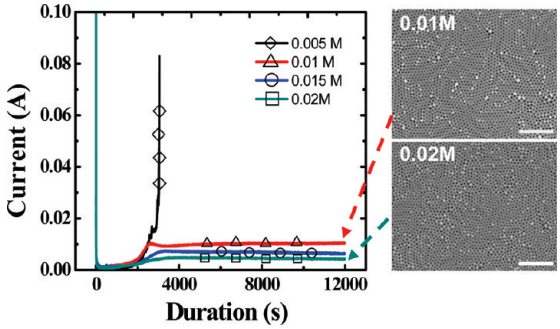

FIGURE 1. Current−time transients during anodization in the electrolyte of 1.0 wt % H_3PO_4 with the addition of 0.005−0.2 M Alox with the first-step anodization (left) and corresponding SEM micrographs of PAA film top surfaces fabricated with the addition of 0.01 and 0.02 M Alox after two-step anodization with the first-step anodization of 6 h (right, scale bar = 5 μm).

current flow (because of the local current concentration) happened along with the film burning in the pore nucleation stage (discussed below). According to the micrographs of scanning electron microscope (SEM, right of Figure 1), the pore and cell in PAA films synthesized in electrolyte with 0.01 M Alox are more even than those from electrolyte with 0.02 M Alox without film breakdown anodized in the same duration, and the aluminum sample is coated by a perfect uniform gray oxide film without any burning spots, whereas lots of dark gray spots with areas of square millimeters appeared on the oxide film surface despite without current catastrophic flow when U_a was increased to 210 V in the case of containing of 0.01 M Alox (see Figure S1 in the Supporting Information). The optimized ratio of H_3PO_4 to Alox at 205 V is also applicable to the U_a of 180−215 V with various concentrations of the electrolyte (see upper left of Figure 2). However, a further increase in U_a at a lower concentration of electrolyte was difficult to obtain.

To explore the limit of U_a, anodic oxidation was performed at 210 V in the electrolyte containing 1.0 wt % H_3PO_4 and 0.02 M Alox. A highly ordered pore arrangement was also obtained without dark gray spots on the film surface, proving that the voltage can be improved with more Alox. On the basis of this finding, the upper limit of U_a was found to be 230 V (D_{int} = 530 nm) in the most diluted solutions (0.27 wt % H_3PO_4 containing 0.0054 M Alox). Further reduction of the concentration of the electrolyte or increase of the amount of Alox cannot improve U_a, because the PAA cannot be obtained as the surface of the aluminum sheet could only be oxidized partially. This may be explained by the lack of the acid, which could not provide enough protons in the anodic oxidation process so that the electric field-assisted dissolution of alumina is restricted.

The dependences of D_{int} and the mass fraction of H_3PO_4 (with the addition of Alox) on U_a are shown in Figure 2. The relationship displays that higher voltages can be employed in more diluted electrolytes with increased D_{int}, similar to what Jagminas et al. (14) reported using various concentrations of H_3PO_4 without any additives; however, it is difficult to form self-ordered PAA in pure H_3PO_4 electrolytes. Previous studies indicated that D_{int} achieved under ordinary MA and HA conditions is linearly dependent on U_a with a

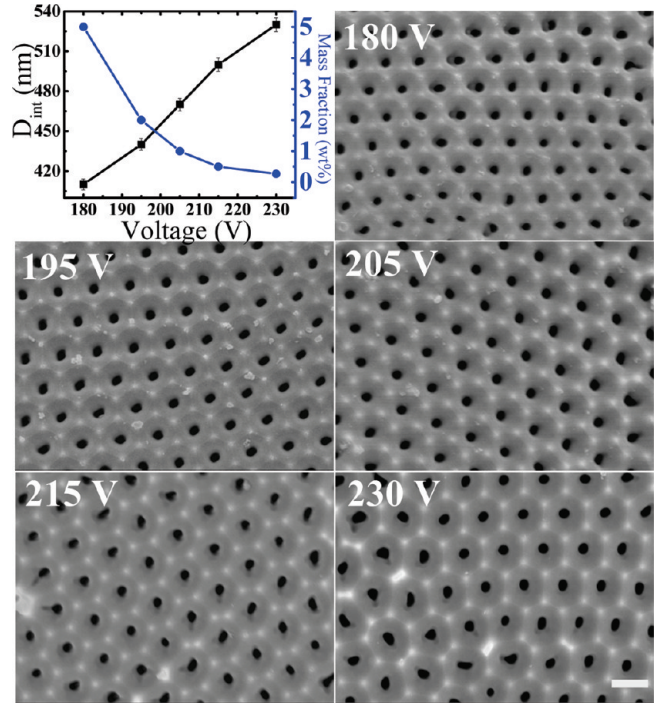

FIGURE 2. The dependences of D_{int} and the mass fraction of H_3PO_4 on U_a (upper left) and corresponding SEM micrographs of PAA top surfaces anodized at U_a =180, 195, 205, 215, and 230 V after two-step anodization with the first-step anodization of 6 h (scale bar = 500 nm).

proportionality constant ζ_{MA} = 2.5 nm V^{-1} and ζ_{HA} = 2.0 nm V^{-1}, respectively (7, 8), whereas the constant ζ_{MA} = 2.3 nm V^{-1}, which is between ζ_{MA} and ζ_{HA}, for PAA in our case is calculated. This value approximates to what Li reported (9), in which the PAA with the D_{int} of 460 nm was prepared in aqueous H_3PO_4 (H_3PO_4:CH_3OH:H_2O = 1:10:89) at 195 V and −4 °C. Digital pixel analysis of the images of SEM shows the porosity of about 5.0 % for our prepared PAA, which are in agreement with the ratio of the pore to cell area via measuring the SEM images. The SEM micrographs of PAA film after proceeding two-step anodization (Figure 2) shows a decreased pore density with an increased U_a, which also indicates the increased D_{int}, and the pore and cell size are uniform in the whole self-organized domains.

The current evolution of PAA films in the mixed electrolyte at U_a = 180−230 V was investigated (Figure 3a). As typical current curves for MA, the growth process has been divided into three stages (15): (a) the barrier layer growth corresponding to the initial current drop stage, (b) the pore nucleation and formation corresponding to the current climb stage, (c) the PAA film growth with pore channel elongated corresponding to the current steady stage. With U_a increasing from 180 to 230 V at the same temperature, stages a and b have been prolonged. This can be explained by the requirement for longer time to form thicker barrier layer with increased U_a, and thus, the dissolution rate of the barrier layer for the pore formation decreases. The duration of stages a and b is shortened with the increase in the anodization temperature, which indirectly proves the explanation above, because the dissolution rate is increased with temperature (see Figure 3b).

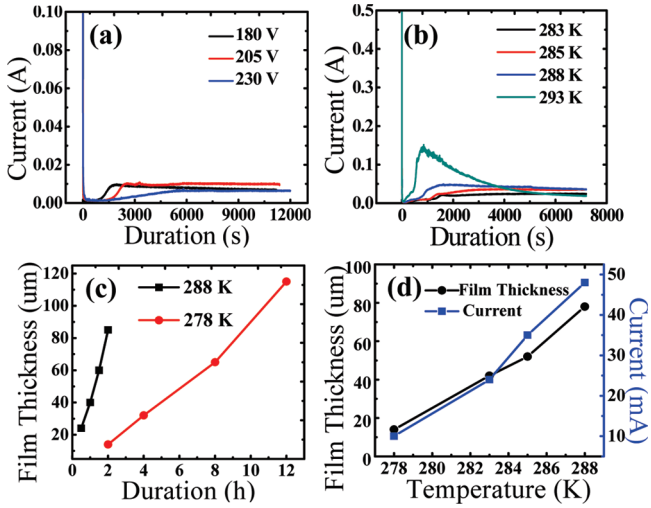

FIGURE 3. Current−time transients during anodization: (a) at the voltage of 180−230 V and 5 °C and (b) at the temperature of 10−20 °C and 205 V. (c) Film thickness as a function of time during anodization at the temperature of 5 and 15 °C and (d) film thickness and current density as a function of temperature anodized at 205 V for 2 h.

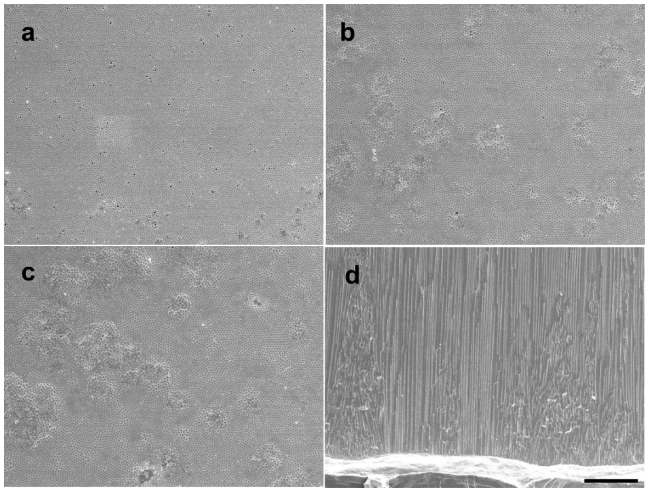

FIGURE 4. SEM micrographs of (a−c) the bottom surface and (d) the cross-section of the PAA film anodized at 205 V and 20 °C for (a) 0.5, (b) 1.5, and (c) 3 h (scale bar = 10 μm).

Notice that the current curve at 20 °C is similar to the current evaluation in the HA process, which is different from the other current curves in Figure 3b. This may reveals that the decrease of current density will occur above a critical current density, which can be attributed to the "diffusion limitation" (8) of the anions in the electrolyte into the pores of PAA films as the PAA film grows much faster with higher current density. The SEM micrographs of the PAA films anodized at 20 °C shown in Figure 4 reveal an interesting phenomenon in the process of PAA film growth. It is shown from Figure 4a−c that the cell arrangement tends to evolve to hexagonal ordered state at the beginning of anodization, whereas as the ordered extent in the ordered domains of PAA cells increase, the defect domains spread and encroach upon the ordered domains, and meanwhile the cells in the defect domains projected out of the bottom surface. The cross-section of the PAA in Figure 4d distinctly reveals the ordered and disordered domains and the process of the defect enlargement. Hebert et al. (16) reported that the average stress of the barrier layer changes from compressive to tensile with increasing current density, that is, the stress of the barrier layer in our case tends to be compressive with decreasing current density, and compressive stress cannot maintain the self-organization state of the PAA. However, the phenomenon of the projection of the defect domains is not understood well.

Panels c and d in Figure 3 show the relationship between the growth rate of PAA films and temperature at 205 V. It should be pointed out that PAA films grow slowly under the typical MA conditions for its low current density, whereas the film growth rate can be increased with current density when the anodization temperature was raised. However, it is difficult to avoid breakdown of PAA films at high potentials and high temperature typically; in our experiments, the problem does not exist at high anodization voltages from 10−20 °C (Figure 3b). The film growth rate is four time faster at 15 °C than that at 5 °C (Figure 3c). When the anodization is performed for 1 h, it has exhibited large domains of the ordered pore arrangement (see Figure S3b in the Supporting Information). From Figure 3d, we can see that the film thickness, proportional to the current, increases with temperature.

Investigations of the ion effects were carried out in the electrolytes of H_3PO_4 added with aluminum phosphate, and the anodic oxidation was not realized even at 0 °C; however, with addition of the same ratio of oxalic acid as Alox, stable anodization was able to proceed at relatively lower temperature, which indicated that the oxalate anions and aluminum cations cooperate with each other at the high potential and temperature, and oxalate ions play the primary role. Whereas aluminum ions, preferring to coordinating with acid anions (oxalate especially), may reduce the ion migration rate, which restrain the anodization process, the formed complexes balance the concentration of protons produced by dissociation of water at the pore bottom, which accelerates the anodization process, and so aluminum ions may act as a buffer with the oxalate together. To learn whether Alox functions in the whole process of anodic oxidation, substitution of 1.0 wt % H_3PO_4 for the mixed solution (1.0 wt % H_3PO_4 and 0.01 M Alox) was done after anodization for 2 h at 205 V. As a result, it lasted no longer than 1 min before the current ascended to a burning level, indicating that Alox works in the whole process.

CONCLUSIONS

In summary, we have obtained self-ordered PAA with D_{int} from 410 to 530 nm in various H_3PO_4 with addition of Alox that is continuously controlled via tuning U_a from 180 to 230 V, and wide temperature region from 5 to 15 °C is applicable. the PAA films with this self-ordered window can be applied to nanofabrication, nano and micro fluidic dynamics and optical materials and so on. Through the typical two-step anodization, ordered pore arrangement with large self-organized domains on both surfaces of PAA films can be achieved. And from the control experiments, we concluded that the aluminum and oxalate ions cooperate with each

other for suppressing breakdown of PAA films in the anodization process.

EXPERIMENTAL SECTION

A typical anodization was carried out in a homemade PTFE cell with samples located on the outside of the wall with a 16 × 16 mm^2 window. Electrolyte temperature was controlled by a snake condenser and the sample temperature was controlled by a thermoelectric solid-state plate equipped with a temperature controller to obtain the real current-temperature relationship during the anodizing process. A graphite plate was used as a cathode. Aluminum sheets (99.999% purity, 0.5 mm thickness) were annealed at 550 °C in the air for 2 h. Then, after removal of the oxide layer of the aluminum surface with sodium hydroxide solution, aluminum sheets were electropolished in perchloric acid/ethanol solution with a volume ratio of 1:4 for 5 min at 20 V and 8 °C. PAA templates were systematically synthesized via a two-step anodization method with U_a values from 180 to 230 V. The first of the two-step anodization was applied to these pretreatment samples for 6 h in 5.0, 2.0, 1.0, 0.5, and 0.27 wt % H_3PO_4 and 0.05, 0.02, 0.01, 0.005, and 0.0054 M Alox at U_a va;ues of 180, 195, 205, 215, and 230 V, respectively,at the anodization temperature of 5 °C (all the temperatures controlled in this letter mean the temperatures of the sample and the electrolytes used). The second anodization was then performed under the same conditions as that of the first anodization after removing the disordered porous oxide film using the solution of 1.8% chromic acid and 6% phosphoric acid. The micrographs of the samples were observed using a field-emission scanning electron microscope (SEM, JSM-6701F). The elemental compositions of PAA films were analyzed by X-ray photoelectron spectroscopy (XPS, AXIS-ULTRA), and the current time transients were monitored by the multimeter of Agilent 34405A.

Acknowledgment. This work was financially supported by the National Natural Science Foundation of China (Grants 50823008 and 20673131) and the "Hundreds Talent Program" of Chinese Academy of Sciences.

Supporting Information Available: Extensive photographs and SEM micrographs of the samples (PDF). This material is available free of charge via the Internet at http://pubs.acs.org.

REFERENCES AND NOTES

(1) Feng, X. D.; Jin, Z. X. *Macromolecules* **2009**, *42* (3), 569–572.
(2) Chen, J. T.; Zhang, M. F.; Russell, T. P. *Nano Lett.* **2007**, *7* (1), 183–187.
(3) Fan, Z. Y.; Razavi, H.; Do, J. W.; Moriwaki, A.; Ergen, O.; Chueh, Y. L.; Leu, P. W.; Ho, J. C.; Takahashi, T.; Reichertz, L. A.; et al. *Nat. Mater.* **2009**, *8* (8), 648–653.
(4) Jani, A. M. M.; Anglin, E. J.; McInnes, S. J. P.; Losic, D.; Shapter, J. G.; Voelcker, N. H. *Chem. Commun.* **2009**, (21), 3062–3064.
(5) Banerjee, P.; Perez, I.; Henn-Lecordier, L.; Lee, S. B.; Rubloff, G. W. *Nat. Nanotechnol.* **2009**, *4* (5), 292–296.
(6) Luo, Z. X.; Liu, Y. Y.; Kang, L. T.; Wang, Y. B.; Fu, H. B.; Ma, Y.; Yao, J. N.; Loo, B. H. *Angew. Chem.Inter. Ed.* **2008**, *47* (46), 8905–8908.
(7) Li, A. P.; Muller, F.; Birner, A.; Nielsch, K.; Gosele, U. *J. Appl. Phys.* **1998**, *84* (11), 6023–6026.
(8) Lee, W.; Ji, R.; Gosele, U.; Nielsch, K. *Nat. Mater.* **2006**, *5* (9), 741–747.
(9) Li, A. P.; Muller, F.; Gosele, U. *Electrochem. Solid-State Lett.* **2000**, *3* (3), 131–134.
(10) Chu, S. Z.; Wada, K.; Inoue, S.; Isogai, M.; Yasumori, A. *Adv. Mater.* **2005**, *17* (17), 2115–2119.
(11) Schwirn, K.; Lee, W.; Hillebrand, R.; Steinhart, M.; Nielsch, K.; Gosele, U. *ACS Nano* **2008**, *2* (2), 302–310.
(12) Li, Y.; Ling, Z. Y.; Chen, S. S.; Cwang, J. *Nanotechnology* **2008**, *19* (22), 25604–25604.
(13) Chen, W.; Wu, J. S.; Xia, X. H. *ACS Nano* **2008**, *2* (5), 959–965.
(14) Jagminas, A.; Bigeliene, D.; Mikulskas, I.; Tomasiunas, R. *J. Cryst. Growth* **2001**, *233* (3), 591–598.
(15) Delloca, C. J.; Fleming, P. J. *J. Electrochem. Soc.* **1976**, *123* (10), 1487–1493.
(16) Hebert, K. R.; Houser, J. E. *J. Electrochem. Soc.* **2009**, *156* (8), C275–C281.

AM1001713